Cellular polarity asymmetrically functionalizes pathogen recognition receptor-mediated intrinsic immune response in human intestinal epithelium cells

Megan L. Stanifer[1,2#], Stephanie Muenchau[1], Kalliopi Pervolaraki[1], Takashi Kanaya[3], Markus Mukenhirn[1], Dorothee Albrecht[1], Charlotte Odendall[4], Jonathan Kagan[5], Sina Bartfeld[6], Hiroshi Ohno[3], Steeve Boulant[1,2#]

[1] Schaller research group at CellNetworks, Department of Infectious Diseases, Virology, Heidelberg University Hospital, Germany;

[2] Research Group "Cellular polarity and viral infection", German Cancer Research Center (DKFZ), Heidelberg, Germany;

[3] Laboratory for Intestinal Ecosystem, RIKEN Center for Integrative Medical Sciences, Yokohama, Kanagawa 230-0045, Japan

[4] Department of Infectious Diseases, King's College London, Guy's Hospital, London SE1 9RT, United Kingdom;

[5] Harvard Medical School and Division of Gastroenterology, Boston Children's Hospital, Boston, MA 02115, USA;

[6] Research Centre for Infectious Diseases, Institute for Molecular Infection Biology, Julius Maximilian University of Wuerzburg, Wuerzburg, Germany

Running Title: Polarized immune response in human intestinal epithelium cells

[#]Corresponding authors

Steeve Boulant, Ph.D.
Department of Infectious Disease, Virology
Schaller research group at CellNetworks and DKFZ
Heidelberg Hospital University
Im Neuenheimer Feld 344
69120 Heidelberg, Germany
Phone: +49 (0) 6221 56 7865
Email: s.boulant@dkfz.de

Megan L. Stanifer, Ph.D.
Department of Infectious Disease, Virology
Heidelberg Hospital University
Im Neuenheimer Feld 344
69120 Heidelberg, Germany
Phone: +49 (0) 6221 56 7858
Email: m.stanifer@dkfz.de

Summary

Intestinal epithelial cells (IECs) act as a physical barrier separating the commensal-containing intestinal tract from the sterile interior. These cells have found a complex balance allowing them to be prepared for pathogen attacks while still tolerating the presence of bacteria and viral stimuli present in the lumen of the gut. Using primary human IECs we probed the mechanisms used by cells to maintain this tolerance. We discovered that stimuli emanating from the basolateral side of IECs elicited a strong induction of the intrinsic immune system as compared to lumenal apical stimulation. Additionally, we determined that this controlled apical response was driven by the clathrin-sorting adapter AP-1B. Mice and human IECs lacking AP-1B showed an exacerbated immune response following apical stimulation. Together these results suggest a model where the cellular polarity program plays an integral role in the ability of IECs to tolerate apical commensals and detect/fight invasive basolateral pathogens.

Keywords: Intrinsic innate immunity, type III interferon, TLR-3, MAVS, cellular polarity, clathrin, AP-1B, lambda interferon, enteric viruses, organoids, intestinal epithelial cells

Introduction

Intestinal epithelial cells (IECs) lining the gastrointestinal tract constitute the primary barrier separating us from the outside environment. The main role of this monolayer of cells is the uptake of nutrients; however, these cells also play a critical role in protecting the human body from enteric bacterial and viral pathogens (Peterson and Artis, 2014). IECs sense and combat pathogen invasions using Pathogen Recognition Receptors (PRRs) to trigger an intrinsic innate immune response, e.g. the Toll-like receptors (TLRs) and RIG-like receptors (RLRs) (Pott and Hornef, 2012, Fukata and Arditi, 2013, Arpaia and Barton, 2011, Barton and Medzhitov, 2003). However, unlike professional immune cells, IECs are in constant contact with the ever-present lumenal microbiota and therefore must have developed mechanisms to tolerate the presence of the commensal bacteria while maintaining responsiveness against pathogen challenges (Fukata and Arditi, 2013). This finely tuned balance has been of interest in the recent years as uncontrolled responses by the epithelium can lead to inflammatory bowel disorders (Pott and Hornef, 2012). The cellular intrinsic innate immune response is regulated not only by complex signal transduction pathways downstream of PRRs but also by compartmentalization of these receptors (Odendall and Kagan, 2017, Chow et al., 2015). This compartmentalization is described to be an important mechanism by which cells avoid self-recognition (Yu and Gao, 2015, Kagan and Barton, 2014). In IECs, this compartmentalization of innate immune functions is believed to be even more critical to control the inflammatory state of cells and to maintain gut homeostasis (Yu and Gao, 2015). IECs are polarized, they display a unique apical membrane facing the lumen of the gut and a basolateral membrane facing the lamina

propria (Yu and Gao, 2015, Rodriguez-Boulan and Macara, 2014). The localization of membrane residing TLRs in IECs has been of interest in recent years. However, due to the complex structure of TLRs, good antibodies have been hard to produce leading to conflicting results over the precise localization of TLRs seen in immunohistochemistry and immunofluorescence stainings of tissues and immortalized IEC lines. To overcome these limitations, a recent study has fluorescently tagged endogenous intestinal TLRs and shown that contrary to past results, many TLRs are found on both the apical and basolateral membrane of epithelial cells form intestine and colon. However, whether the TLRs located at the apical vs. the basolateral plasma membrane of these epithelial cells display similar downstream signaling and induced pro-inflammatory response remains to be determined (Price et al., 2018).

While the polarized localization of TLRs specialized in sensing bacteria and their activation has been explored in IECs, how viruses are detected and combatted in the human intestinal epithelium has been largely understudied. Similarly, whether PRRs specialized in sensing viruses and whether other PRRs specialized in sensing cytosolic pathogen associated molecular pattern (PAMPs) (e.g. RLRs) also display a polarized intracellular location within IECs to adapt their response to the side of viral pathogen challenge (apical *vs.* basolateral) remains to be carefully addressed.

In our study, using human derived intestinal organoids, we investigated whether intestinal epithelial cells could distinguish viral infections emanating from either the apical or basolateral membrane. We determined that the viral ability to replicate and produce progeny virions was side specific. We observed

that an apical infection leads to a greater production of *de novo* viruses compared to a basolateral infection. Concomitantly, we found that a basolateral infection leads to a higher intrinsic innate immune response compared to an apical infection. Importantly, this higher basolateral innate immune induction appears to be a general mechanism as it was neither cell type, virus nor pathogen associated molecular pattern specific. Using mouse derived organoids and knock-down approaches, we determined that mechanisms leading to the establishment of cellular polarity in IECs were key to control the observed polarized immune response. This discovery of a global polarized immune response strongly suggests a universal mechanism used by intestinal epithelial cells to generate (1) a moderate immune response against microbe stimuli (bacterial and viral) emanating from the physiological lumenal side while (2) remaining fully responsive against invasive pathogens or in conditions of barrier integrity loss where stimuli can access the normally sterile basolateral side.

Results

Apical infection of human IECs leads to more *de novo* virus production compared to basolateral infection. Human intestinal epithelial cells (hIECs) are polarized with an apical and basolateral membrane separated by tight junctions (Weisz and Rodriguez-Boulan, 2009). Enteric pathogens and commensals are normally located in the lumen of the gut thereby generally challenging hIECs through their apical membrane. However, in some circumstances, gut lesions and loss of barrier functions of the gut epithelium can allow lumenal microbes to pass the protective epithelium gaining access to the basolateral side of hIECs. Alternatively, microbes, particularly enteric viruses can be transcytosed by M cells allowing them to initiate infection from the basolateral of hIECs (Wolf et al., 1981). To investigate whether the side of infection of hIECs by viruses can impact the outcome of infection, replication, and spread, we seeded human colon carcinoma-derived IECs, T84 cells, on transwell inserts and allowed them to polarize and to form a tight epithelium-like monolayer. As we previously reported (Stanifer et al., 2016), we confirmed that these cells were polarized and display a full barrier function. Trans-Epithelium Electrical Resistance (TEER) monitoring, which provides a measurement of cellular monolayer tightness, showed that T84 cells reached their polarized level (Madara et al., 1987) (1000 Ohm/cm^2) in five days post-seeding (Sup. Figure 1A). This polarized phenotype was confirmed by monitoring the integrity of the tight junction belt through immunostaining of the tight junction protein ZO-1 (Sup. Figure 1B); and by controlling the capacity of a monolayer of polarized T84 cells to block dextran diffusion from the apical to the

basolateral chamber in a transwell diffusion assay (Sup. Figure 1C).

Polarized T84 cells were infected either apically or basolaterally with mammalian reovirus (MRV), a model enteric virus (Figure 1A). Previous work in our lab has shown that the polarized nature of infected cells is maintained for several days post-infection (Stanifer et al., 2016). Immunostaining of the tight junction belt and TEER measurements further confirmed that infection by MRV did not disrupt the polarized nature of the cells (Sup. Figure 1A-B). MRV infection was followed over time by qRT-PCR of the MRV genome, as well as Western blot and immunofluorescence (IF) staining for the non-structural viral protein μNS (Figure 1B-D). Results show that infection of T84 cells initiated with a similar kinetics when cells where infected by MRV from their apical or basolateral side (Figure 1B-D). However, while IF staining revealed that the same number of cells were infected from both an apical or basolateral infection (Sup. Figure 1B and Figure 1B), quantification of virus replication by Western blot showed that an apical infection produced a larger quantity of the viral non-structural protein μNS at 24 hours post-infection (hpi) (Figure 1C). To determine if this excess μNS correlated with increased *de novo* viral production, T84 cells were infected with MRV apically or basolaterally and cells were collected in 24-hour intervals over four days. Virus production was then assayed by plaque assay and revealed that an apical infection lead to a higher production of *de novo* viral particles compared to a basolateral infection (Figure 1E).

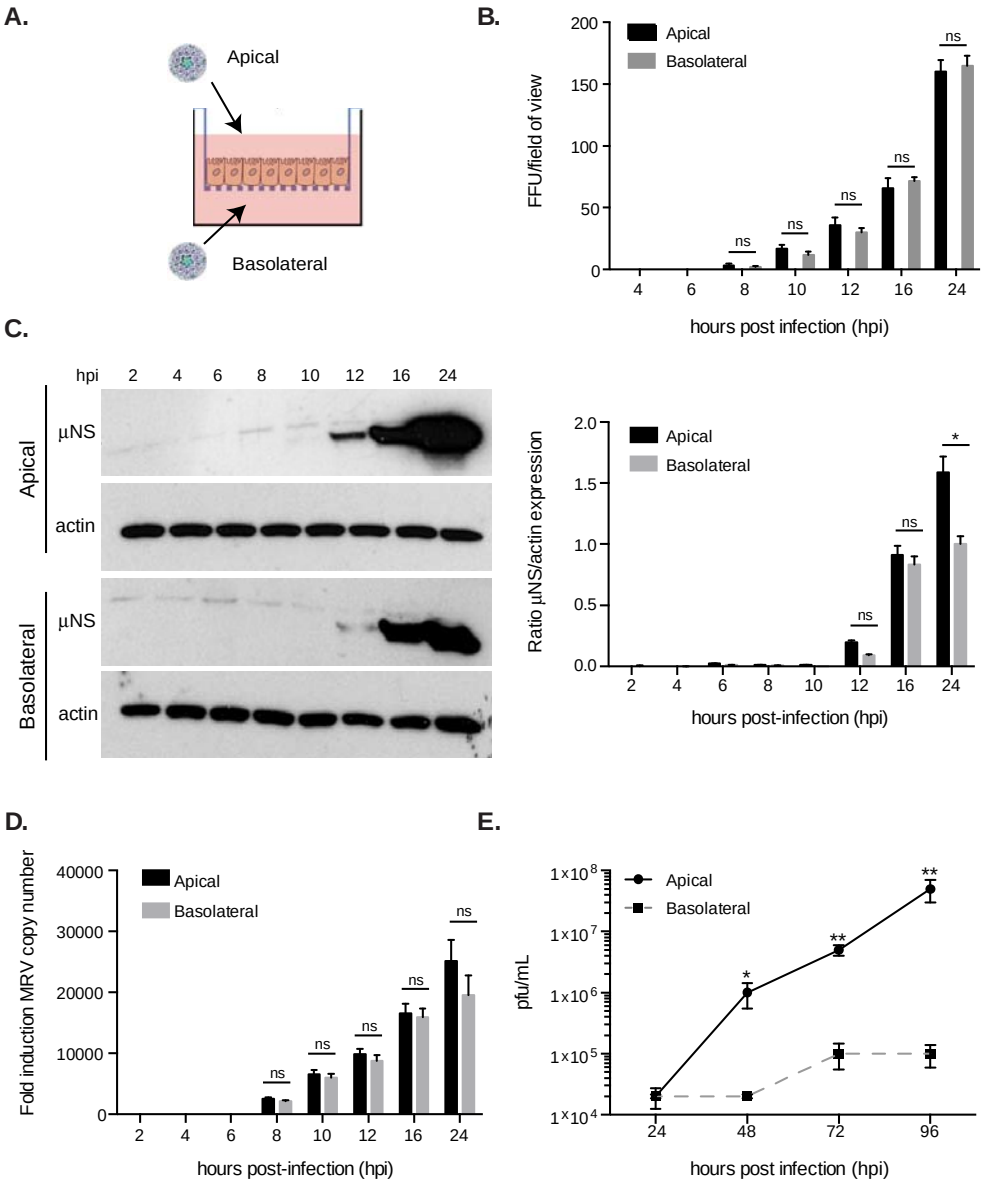

Figure 1. Apical infection leads to more *de novo* MRV virus production compared to basolateral infection. Polarized T84 cells were infected apically or basolaterally with MRV. (A). Schematic showing polarized cells grown on a transwell insert allowing us to access the apical and basolateral sides independently. (B). Infected cells were fixed at indicated time points and indirect immunofluorescence was performed against the non-structural protein µNS. 10 fields of view were counted for each time point. (C). Same as B except protein samples were subjected to Western blot of the MRV non-structural protein µNS. Actin was used as a loading control. Representative figure is shown. (D). Infected cells were collected at the indicated time points and RNA samples were assayed for the production of the MRV µ2 genome segment. (E). Infected cells and supernatants were collected in 24 hour intervals for five days. Samples were freeze/thawed and total *de novo* virus production was assessed by plaque assay. (B-E) Experiments were performed in triplicate, error bars indicate the standard deviation. ns=not significant , *<P.05, **P < 0.01 (unpaired t-test)

Polarized hIECS have a higher innate immune induction characterized by a prolonged type III IFN expression from basolateral infection/stimulation. Our results indicate that T84 cells can equally support infection from both their apical and basolateral membranes. However, over time, *de novo* virus production appears to be more constrained upon basolateral infection. We therefore investigated the source of this basolateral restriction and evaluated whether the intrinsic innate immune response generated by hIECs was different when infection emanated from their apical *vs.* their basolateral side. T84 cells were infected with MRV from their apical or basolateral side and their intrinsic innate immune response was monitored as we previously reported by evaluating the induction of either type I IFN (IFNβ1) or type III IFN (INFλ2/3) 16 hpi by q-RT-PCR (Stanifer et al., 2016, Pervolaraki et al., 2017). Results showed that although there was a similar level of virus infectivity with a similar number of infected cells at early times post-infection (Figure 2A and Sup. Figure 2A), there was a significantly higher production of both IFNβ1 and INFλ2/3 transcripts following a basolateral infection compared to an apical one (Figure 2A). Using an additional hIEC cell line, SKCO15 cells (Le Bivic et al., 1989), we confirmed that this phenotype was not cell type specific (Sup. Figure 2B-C). To verify that this phenotype was neither MRV nor virus specific, we infected our T84 cells in a polarized manner with *Encephalomyocarditisvirus* (EMCV) Mengovirus (Mengo) and *Salmonella enterica serovar typhimurium (*StM*)*. Using indirect immunofluorescence, we confirmed that similar to MRV, Mengo and *S.* Typhimurium could equally infect T84 cells from their apical or basolateral sides (Figure 2B-C and Sup. Figure 2A). Interestingly, when either Mengo or *S.* Typhimurium infected cells were evaluated for their intrinsic innate immune

induction, we could show that a basolateral infection lead to a stronger production of both IFNβ1 and INFλ2/3 compared to an apical infection (Figure 2B-C).

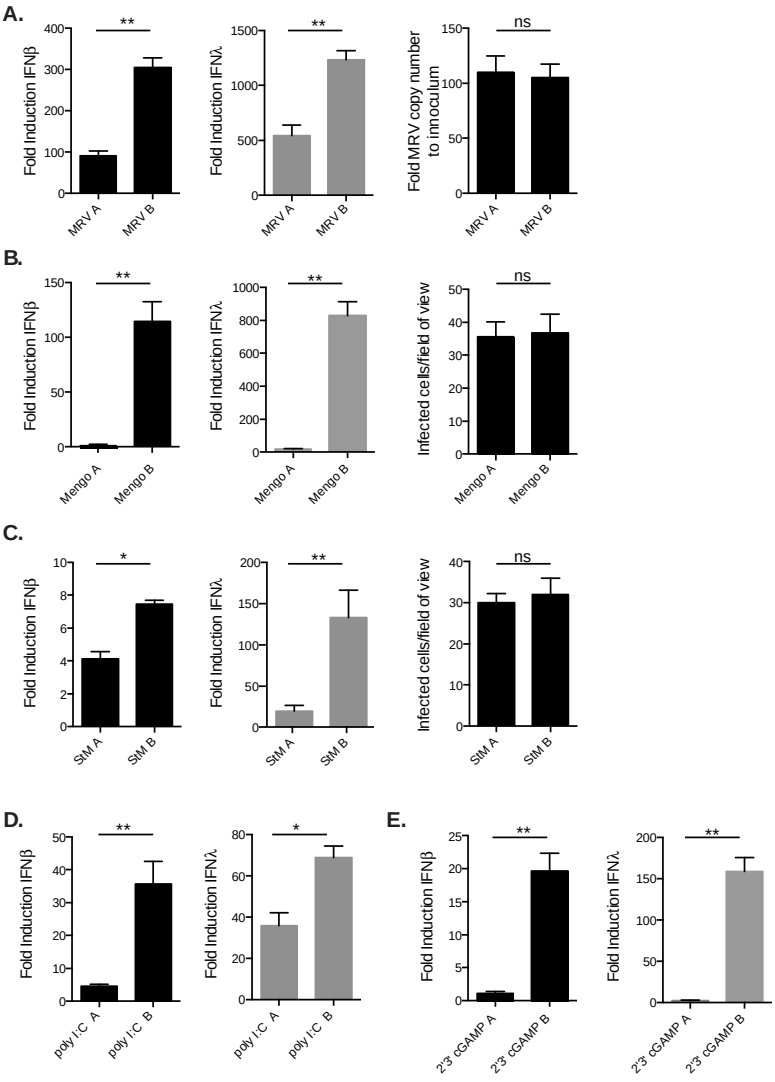

Figure 2. Basolateral stimulation leads to a higher induction of both type I and III interferons. T84 cells were seeded onto transwell inserts until they reached a polarized state. (A). T84 cells were infected with MRV either apically or basolaterally for 16h. Samples were collected and the induction of the intrinsic innate immune system was analyzed by qPCR for type I (IFNβ) or type III (INFλ2/3) IFNs. Viral infection was determined by indirect immunofluorescence against the MRV non-structural protein μNS. (B) Same as A except using EMCV Mengo. (C). Same as A except using *Salmonella*-mCherry (StM) and analyzing samples 8 hpi. (D) T84 cells were transfected apically or basolaterally with poly I:C. RNA was harvested and analyzed 6 hours post-treatment. (E) 2'3'cGAMP was added either to the apical or basolateral side of polarized T84 cells. RNA was harvested and analyzed 6 hours post-treatment. (A-E). All experiments were performed in triplicate. Error bars indicate the standard deviation. ns=not significant, *<P.05, **P < 0.01 (unpaired t-test).

As pathogens often have mechanisms to interfere with the intrinsic innate immune response, we wanted to confirm that our polarized immune response was not the result of different inhibitory mechanisms developed by pathogens as a function of the entry side. For this we used transfected poly I:C, a mimicry of dsRNA commonly used to stimulate the Rig-Like receptor (RLR) pathway. Stimulation of polarized T84 cells with poly I:C revealed that the amplitude of the immune response was dependent on the treatment side. Cells stimulated from their basolateral side displayed a greater production of IFN compared to cells stimulated from their apical side (Figure 2D). Similarly, we used the synthetic analogs 2'3'cGAMP mimicking infection by a DNA virus or bacteria to specifically activate the STING pathway and could further confirm that T84 cells generate a polarized innate immune response. (Figure 2E). These results indicate that polarized T84 cells have an intrinsic mechanism allowing them to distinguish between invading pathogens or stimuli (PAMPs) emanating from their apical or basolateral side and, most importantly, that they can adapt their response to the entry side.

Primary intestinal cells show a higher intrinsic immune response to viral stimuli. T84 cells are immortalized carcinoma derived cells. Due to their cancerous nature, they are likely to display altered signal transduction pathways. Therefore, we then turned to non-transformed human mini-gut organoids to validate our findings in human primary cells. We have previously shown that human mini-gut organoids can be infected by MRV and mount an immune response which is characterized by the upregulation of both IFNβ1 and INFλ2/3 (Pervolaraki et al., 2017). Human mini-gut organoids are large multi-

cellular structures, with the apical membrane of hIECs facing the lumenal interior and their basolateral membrane facing the exterior environment. Using microinjection, MRV was introduced within the organoids to allow for apical infection or juxtaposed at the organoid periphery to promote basolateral infection (Figure 3A). We first validated that our apical and basolateral microinjection approaches led to equivalent infection of the human mini-gut organoids as controlled by western blot analysis against the MRV non-structural protein μNS and qRT-PCR of the viral genome (Figure 3B-C, right panel). Similar to our T84 cells, human mini-gut organoids also displayed a polarized immune response as shown by a higher induction of both IFNβ1 and INFλ2/3 transcripts following basolateral infection (Figure 3C).

Due to their 3D nature, it is difficult to fully address, in organoids, the number of cells that get infected upon apical and basolateral infection. As such, we implemented a method to create a 2D monolayer out of the human mini-gut organoids (Figure 3D) (see method section for details). This allowed us to grow our mini-guts on transwell inserts thereby allowing us to gain specific and precise access to their apical or basolateral side independently. Primary hIECs grown on transwells were able to polarize as shown by the formation of a complete tight junction belt (ZO-1 staining, Figure 3E) and by the establishment of barrier function as measured by TEER (data not shown). These polarized primary hIECs were infected with MRV from their apical or basolateral side. Transcript analysis and immunostaining of the non-structural protein μNS showed that while infection levels were independent of the side of infection (Figure 3F, right panel), basolateral infection led to a higher induction of both

IFNβ1 and INFλ2/3 (Figure 3F) confirming the results obtained both using microinjection of organoids (Figure 3C) and in T84 cells (Figure 2A). All together

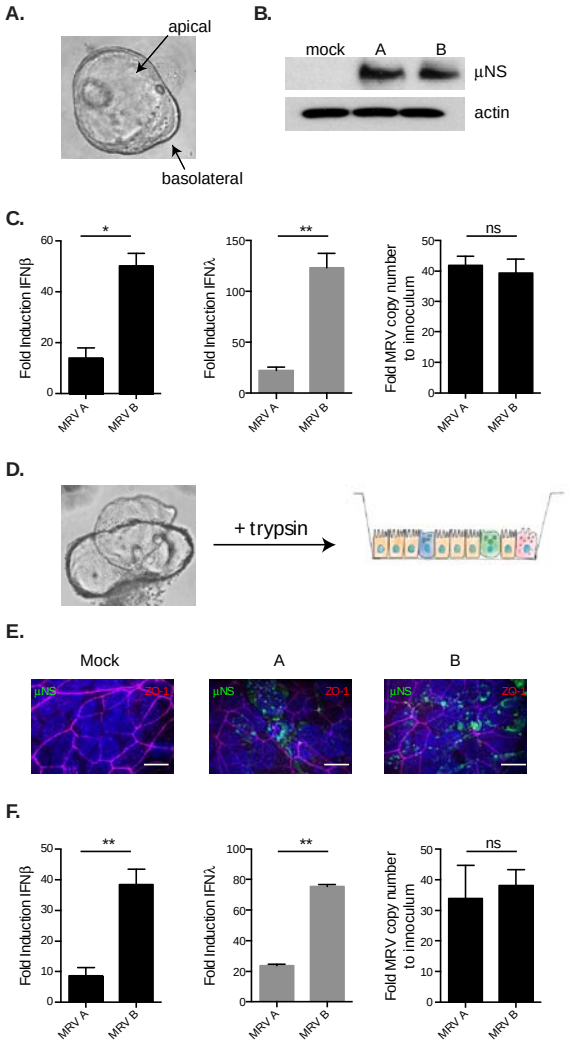

Figure 3. Human organoids display a polarized intrinsic immune response. (A) Schematic of the microinjection approach used to infect organoids specifically from either their apical or basolateral sides. (B-C) Human intestinal organoids were infected by MRV apically or basolaterally through microinjection. Virus infection was assessed 16 hpi for (B) the production of the non-structural viral protein µNS using Western blot analysis and (C) for the production of an intrinsic immune induction by quantifying the production of type I (IFNβ) and type III (IFNλ2/3) interferons using qPCR. (D) Human colon organoids were seeded onto transwells and allowed to polarize for five days (see method for details). Polarized monolayers were infected with MRV apically or basolaterally and assessed 16 hpi for (E) viral infection and polarization by indirect immunofluorescence (green= µNS, red=ZO-1, blue=DAPI) and (F) for the production of an intrinsic immune induction by quantifying the production of type I (IFNβ) and type III (IFNλ2/3) interferons using qPCR. (B-F) All experiments were performed in triplicate. Representative immunofluorescence and western blot are shown. Error bars indicate the standard deviation. Scale bar =10µM. ns=not significant, *<P.05, **P < 0.01 (unpaired t-test).

these results demonstrate that human intestinal epithelial cells have developed mechanisms allowing them to generate a stronger innate immune response following stimulation emanating from their basolateral side compared to apical stimuli.

Basolateral infection leads to prolonged production of type III IFN. To evaluate the duration of this polarized response, polarized hIECs were infected with MRV and the upregulation of both IFNβ1 and INFλ2/3 transcripts was evaluated over time. We found that an apical infection led to a rapid up and down regulation of both IFNβ1 and INFλ2/3 transcripts (Figure 4A). Interestingly, we found that a basolateral infection also showed this same quick up and down regulation of the IFNβ1 transcript, however expression of INFλ2/3 transcript was sustained over time (Figure 4A). To confirm that the prolonged INFλ2/3 expression was also shown at the protein level, T84 cells were infected from either their apical or basolateral membrane and supernatants were collected over time for ELISA analysis (Stanifer et al., 2016). Our ELISA results confirm that an apical infection leads to an acute INFλ2/3 production and secretion while a basolateral infection leads to a greater and prolonged production and secretion of INFλ2/3 (Figure 4B). This prolonged INFλ2/3 expression upon basolateral stimulation was also observed in cells treated with both poly I:C and cGAMP (Sup. Figure 3A-B, respectively). As this apparent prolonged production of type III IFN transcript could be due to a sustained transcriptional activity or an increased RNA stability, cells were treated with actinomycin to inhibit new RNA synthesis (Sup. Figure 4A). Upon actinomycin treatment, basolateral challenges produced IFNβ1 and INFλ2/3 transcripts

277 whose half-life were slightly shorter than apical infections arguing that the
278 stronger immune response generated upon basolateral challenges is not the
279 results of differences in the stability of the IFN transcripts (Sup. Figure 4B). This
280 strongly suggests that an apical and a basolateral infection lead to different
281 transcriptional activities of IFNs with a basolateral infection leading to a
282 prolonged transcription of INFλ2/3.

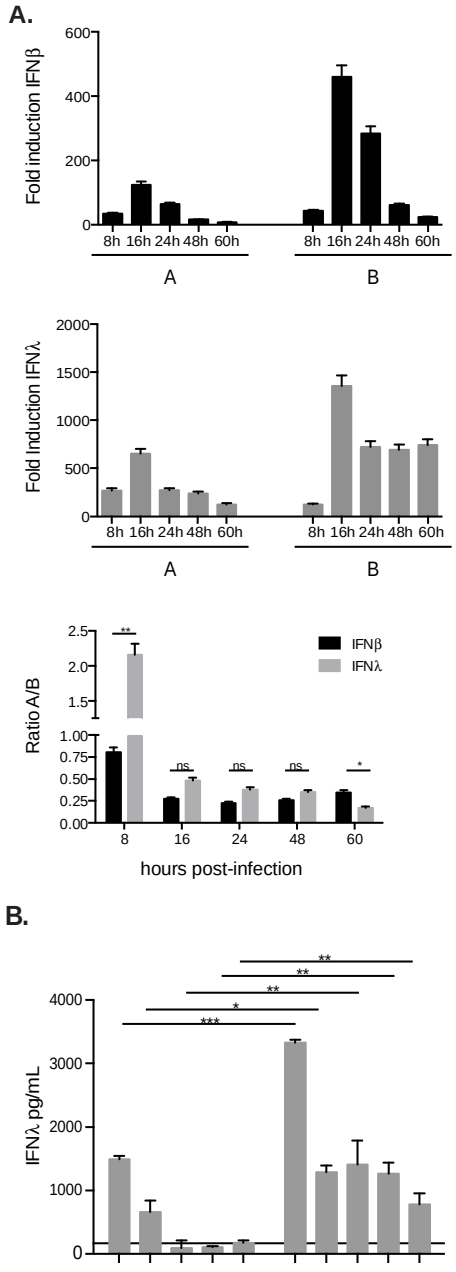

Figure 4. Basolateral infection leads to a prolonged production of type III interferon. (A) Polarized T84 cells were infected apically or basolaterally with MRV. RNA samples were collected at the indicated times post-infection and analyzed by qPCR for the intrinsic innate immune induction of type I (IFNβ) and type III (IFNλ2/3) interferons. (B). Polarized T84 cells were infected apically or basolaterally with MRV. Supernatants from the basolateral side were collected at the indicated times post-infection and analyzed by ELISA for the secretion of type III (IFNλ2/3) interferon. A=apical infection, basolateral supernatant. B =basolateral infection/basolateral supernatant (Stanifer et al., 2016). Black line indicates limit of detection. (A-B) All samples were performed in triplicate. Error bars indicate the standard deviation. ns=not significant, *<P.05, **P < 0.01, ***P < 0.001 (unpaired t-test).

All together these results show that hIECs can detect pathogens entering from both their apical and basolateral sides but that basolateral stimulation induces a larger and sustained intrinsic immune response characterized by a greater production and secretion of type III IFNs.

Apical stimulation of hIECs generates a negative signal, which down regulates the intrinsic innate immune response. Our above results indicate that an apical infection is efficiently detected by hIECs and leads to the generation of an intrinsic innate immune response. However, opposite to basolateral stimulation, this response is quickly downregulated (Figure 4). To gain insight on the mechanism leading to this downregulation of immune response, cells were co-infected from both sides and immune response was compared to the one generated upon unilateral infection conditions. Immunofluorescence staining confirmed that a dual infection leads to an increased number of infected cells (Sup. Figure 5A-B). However, results show that co-infection of cells from their apical and basolateral side does not lead to an additive immune-stimulatory effect, but on the contrary, leads to a dampening of the immune induction compared to basolateral infection only (Sup. Figure 5C). These results show that while apical infection induces an acute immune response in hIECs, it is quickly followed by a global negative feedback signal which leads to the down regulation of the intrinsic innate immune response.

The clathrin adapter AP-1B-mediated cellular polarity drives polarized immune response in IECs Our observations made both in immortalized carcinoma derived cell lines and in primary human IECs demonstrate that polarized intestinal epithelial cells are able to distinguish and to adjust their

intrinsic innate immune response in a side dependent manner. Viral infection or pathogen challenges emanating from the basolateral side leads to a stronger immune response compared to apical stimuli. To identify the mechanisms driving this polarized immune response we reasoned that this unique response is intrinsically linked to the polarized nature of IECs. The apical and basolateral membranes are established through the coordinated sorting of both proteins and lipids, the polarization of both the actin and microtubule cytoskeleton, and the creation of a tight junction belt (Weisz and Rodriguez-Boulan, 2009, Gonzalez and Rodriguez-Boulan, 2009). Proteins are polarized due to unique sorting signals such as YXXØ (where Ø represents amino acids with a bulky hydrophobic side chain), NPXY and DXXLL for basolateral cargo or GPI anchors and modified transmembrane or cytosolic domains for apical cargo (De Matteis and Luini, 2008). Currently the best-characterized basolateral sorting machinery is AP-1, which comes in two forms; the ubiquitously expressed AP-1A and the epithelial specific AP-1B. AP-1B has been described as being localized to the recycling endosomes (RE) and is a key protein involved in sorting proteins from the RE to the basolateral membrane (Folsch, 2015). Interestingly, AP-1B knock-out mice not only suffer from the loss of basolateral polarization (Hase et al., 2013) but also display an uncontrolled inflammatory response in the intestinal tract in the absence of infection (Takahashi et al., 2011).

To determine if AP-1B also played a role in pathogen induced sensing we created a T84 cell line in which AP-1B was depleted by shRNA against the μ1b subunit (AP-1B kd) (Sup. Figure 6A). TEER measurements and ZO-1 staining confirmed that T84 cells depleted of AP-1B maintained their tight junction

integrity (Sup. Figure 6B-C) (Gonzalez and Rodriguez-Boulan, 2009). These AP-1B knock-down cell lines were then seeded onto transwell inserts and challenged with MRV either from their apical or basolateral side. Interestingly, apical infection of the AP-1B knock-down cell lines lead to an exacerbated and prolonged INFλ2/3 production compared to wild type cells (Figure 5A). Similar results were found when monitoring INFβ1 (data not shown). The increased production of type III interferon upon apical infection was also seen at the protein level through increased INFλ2/3 secretion into the supernatants (Sup. Figure 6D). These results strongly indicate that AP-1B is responsible for the polarized immune response observed in our hIECs during MRV infection.

Importantly, to determine whether the increased innate immune induction upon apical stimulation was based on initial virus sensing or due to downstream interferon signaling, WT and AP-1B knock-down T84 cells were treated apically or basolaterally with either IFNβ or IFNλ. Results showed that IFNλ activates STAT-1 phosphorylation and ISG production through both apical and basolateral stimulation. Importantly, this was unaltered when AP-1B was knocked-down (Sup. Figure 6E). Additionally, IFNβ1 stimulation shows a polarized induction of immune response, with basolateral stimulation producing a much higher STAT-1 phosphorylation and ISG production, this was also unchanged when AP-1B was knocked-down strongly suggesting that AP-1B is acting on the level of virus sensing.

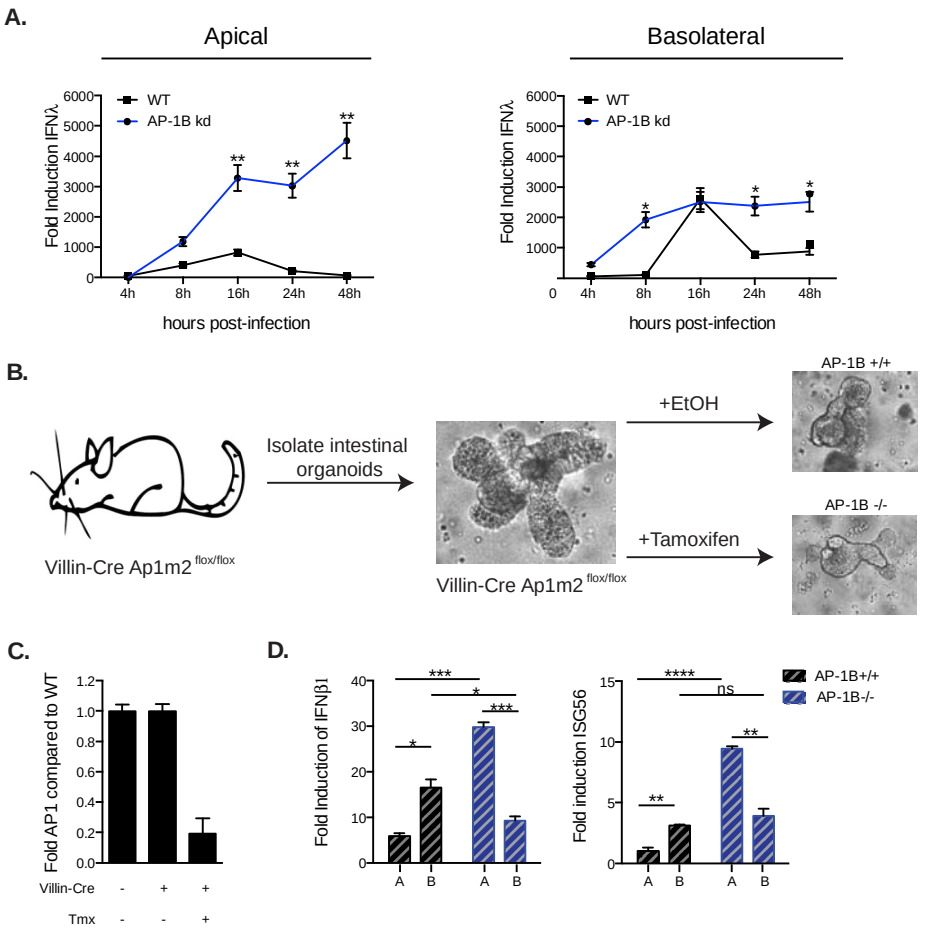

Figure 5. AP-1B-mediated cellular polarity controls the polarized immune response. (A) WT and AP-1B knock-down T84 cells were polarized on transwell inserts. Cells were infected with MRV apically or basolaterally. RNA samples were harvested at indicated time points post-infection and the intrinsic innate immune induction was analyzed by qPCR for type III (IFNλ2/3) interferon. (B) Schematic for the generation of the inducible murine AP-1B knock-out organoids. (C). AP-1B knock-out was controlled by qPCR for exon 4-5 of the Ap1m2 locus. (D) Non-tamoxifen treated Cre mice (AP-1B+/+) or AP-1B -/- mouse organoids were seeded onto transwells and infected with MRV in a polarized manner. 48 hours post-infection cells were harvested and analyzed for the induction of IFNβ1 and ISG56 by qRT-PCR. All experiments were performed in triplicate. Error bars indicate the standard deviation. ns=not significant, *<P.05, **P < 0.01, *** P < 0.001, *** P < 0.0001 (unpaired t-test).

354

355 To confirm that AP-1B was contributing to the observed polarized
356 immune response we evaluated mice, which express an inducible intestinal
357 specific knock-out of AP-1B (villin-Cre-Ap1m2$^{flox/flox}$, (Takahashi et al., 2011))
358 (Figure 5B). Intestinal organoids were generated from these mice as polarized

infection is not possible using intact mice. While apical infection can be mimicked through gavaging of virus, basolateral infection cannot be controlled as intraperitoneal infection will also deliver virus to the surrounding immune cells and stroma cells thereby resulting in an immune response generated not only by IECs but also by other cell types. Organoids generated from villin-Cre-Ap1m2$^{flox/flox}$ were treated with or without tamoxifen and the loss of AP-1B was controlled by qPCR (Figure 5C) (see method). AP-1B$^{+/+}$ and AP-1B$^{-/-}$ organoids were seeded onto transwells and infected apically or basolaterally with MRV. The innate immune induction was controlled by q-RT-PCR and confirmed that similar to our T84 cell model and to our human organoids, murine organoids also show a polarized immune response where a basolateral stimulation leads to a stronger production of IFN compared to an apical one (Figure 5D). Most importantly, organoids derived from AP-1B floxed mice also display an inversion in their polarized immune response upon tamoxifen-induced knock-out of AP-1B. Indeed, apical infection leads to the expression of higher amounts of IFN and interferon stimulated genes compared to organoids derived from WT mice (data not shown) or to the Ap1b$^{+/+}$ (floxed non-tamoxifen treated organoids) (Figure 5D).

All together these results indicate that in the absence of AP-1B, response emanating from an apical stimuli is exacerbated. This highlights the key role of the AP-1-mediated cellular polarity in regulating intrinsic innate immune response in IECs.

AP-1B mediated sorting is responsible for the TLR3-mediated polarized immune response. We and others have previously demonstrated that MRV is

383 detected by both the RLRs MDA-5 and RIG-I as well as TLR3 (Stanifer et al., 2016,
384 Loo et al., 2008). To determine if AP-1B establishes a polarized immune response
385 through sorting of RLRs and/or TLRs, we infected polarized T84 WT or AP-1B
386 knock-down cells with Mengo virus, which is known to activate its immune
387 response through the RLR pathway only (Feng et al., 2012). Unlike during MRV
388 infection, apical infection of AP-1B knock-down cells by Mengo viruses did not
389 lead to a stronger immune response compared to a basolateral infection. In other
390 words, the innate immune induction of Mengo infected cells was unaltered in AP-
391 1B knock-down cells compared to wild type cells (Figure 6A). Similarly,
392 transfected poly I:C induced a similar production of INFλ2/3 in both wild type
393 and AP-1B knock-down cells (Figure 6B) and activation of STING by cGAMP was
394 also unaffected by AP-1B depletion (data not shown). These findings
395 demonstrate that the AP-1 recycling machinery is not involved in the functional
396 polarization of RLRs and STING.

397 The above results strongly suggest a model where the moderate and
398 controlled immune response observed upon apical viral infection is highly
399 dependent on TLR3 signaling. TLR3 requires TRIF as adapter protein to mediate
400 downstream signaling (Yamamoto et al., 2003). To address whether the antiviral
401 innate immune response generated hIECs upon viral infection from their apical
402 side is due to TLR3, we treated our polarized WT T84 cells with an inhibitor of
403 TRIF, thereby blocking TLR3-mediated immune response, and subsequently
404 infected them in a polarized manner with MRV. In the presence of the TRIF
405 inhibitor, production of INFλ2/3 was strongly reduced in WT cells infected from
406 their apical side (Figure 6C, left panel). Similarly, results show that TLR3 was

also responsible for sensing MRV infection emanating from the basolateral side of hIECs, but to a lesser extent compared to an apical infection (Figure 6C, right panel). Similar results were found when monitoring INFβ1 (data not shown). This strongly suggests that RLRs and TLR3 might both be responsible for the antiviral signaling observed during basolateral infection while TLR3 might be the predominant sensing pathway of an apical viral infection.

To directly challenge this hypothesis, we exploited our AP-1B knock-down cells and addressed whether the exacerbated immune response observed upon apical infection of hIECs (Figure 5) was driven by TLR3. AP-1B knock-down cells were infected apically or basolaterally with MRV in the presence or absence of the TRIF inhibitor, and the induction of INFλ2/3 transcripts was followed over time by q-RT-PCR. Remarkably, while infection of AP-1B knock-down cells from their apical side leads to an exacerbated immune response, the presence of the TRIF inhibitor results in significant decrease of immune response almost comparable to the levels observed in WT cells (Figure 6D). These findings strongly suggest that the exacerbated immune response observed in AP-1B knock down cells is mediated by TLR3. All together these data support a model where the clathrin sorting adaptor AP-1B allows for the functional polarization of TLR3 allowing hIECs to mount a side specific immune response upon viral infection.

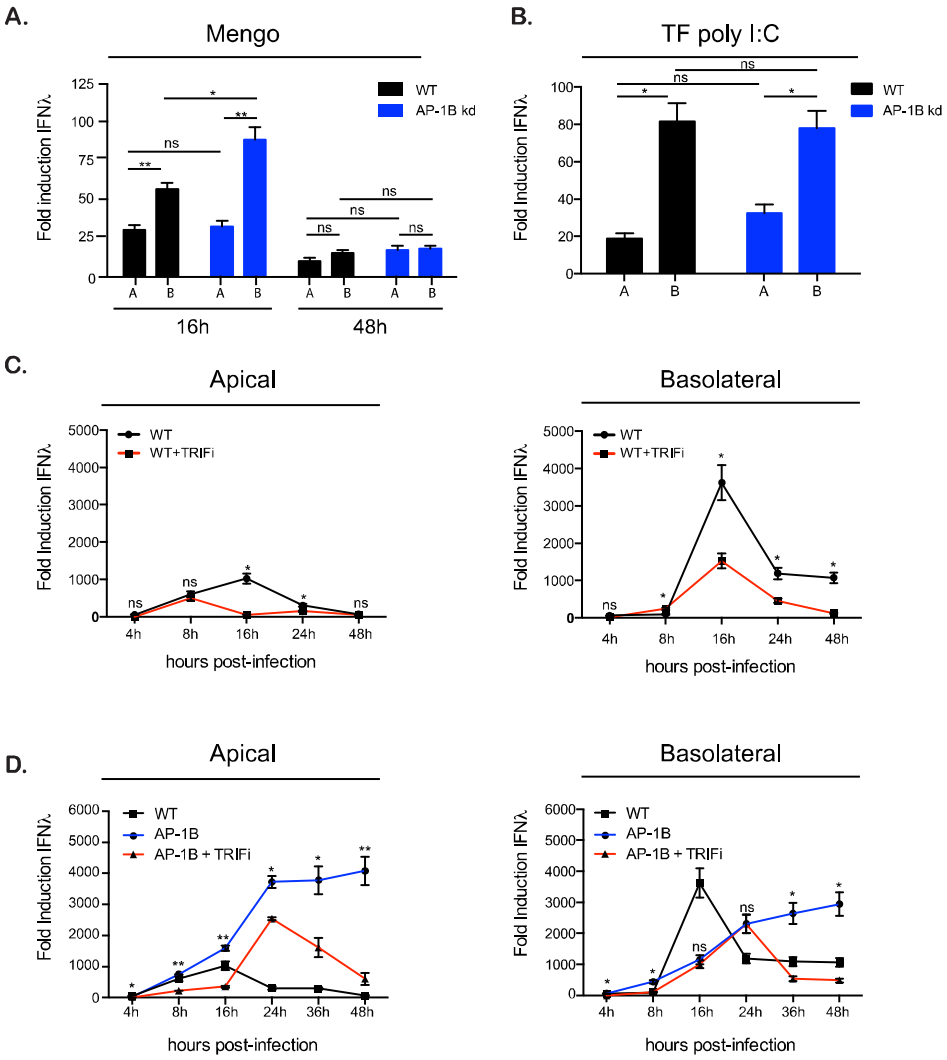

Figure 6. AP-1-mediated cellular polarity shapes TLR3 driven immune response. (A). WT and AP-1B knock-down T84 cells were polarized on transwell inserts. Cells were infected with EMCV Mengovirus and harvested at 16 and 48 hpi and analyzed for intrinsic immune induction of type III IFNs by qRT-PCR. (B) Same as A except cells were transfected with poly I:C and harvested at 12 hours post-treatment. (C-D) Cells were treated with a TRIF inhibitor or a control peptide. RNA samples were harvested at indicated time points post-MRV infection and the intrinsic innate immune induction was analyzed by qPCR for type III (IFNλ2/3) interferons. (C) WT cells (D) AP-1B kd cells. (A-D). All experiments were performed in triplicate. Error bars indicate the standard deviation. ns=not significant, * $P < 0.05$. ** $P < 0.01$. Statistics in panel D are between AP-1B and AP-1B+TRIF.

430

431

432

433

Discussion

The microbial content present in the lumen of gut represents a colossal challenge for IECs lining our gastrointestinal tract. On one hand, they need to cohabitate to exploit the benefit that the commensal flora brings to the host, but on the other hand, they need to remain immune responsive to deal with potential pathogens (Pott and Hornef, 2012). In this study we show that polarized IECs can distinguish between pathogen challenges emanating from their apical or basolateral side. We unraveled that the extent of the immune response which is generated downstream both endosomal and cytosolic PRRs depends on the side (apical vs. basolateral) of infection/stimulation. Precisely, we show that basolateral infection/stimulation leads to a higher induction and secretion of INFλ2/3 compared to an apical infection. We identified the clathrin adaptor AP-1B sorting machinery as a key player driving the polarized innate immune response in IECs upon viral infection. We show that the AP-1B sorting machinery allows for the asymmetric functional polarization of TLR3, allowing IECs to be more responsive from their basolateral side. Interference with this sorting mechanism renders IECs more sensitive to apical stimuli. We propose that the polarized immune response generated by IECs against the broad range of PAMPs and pathogens represents a unique immune-strategy to create a homeostatic interface between the microbiota and the intestinal epithelial barrier. It allows IECs to restrain their immune response against the naturally present apical stimuli while remaining fully responsive to infection/stimulation emanating from the physiologically sterile basolateral side, which will only be accessible during loss of barrier function or during infection by invasive pathogens.

Only a few studies have tried to correlate the specific localization of TLRs at the apical and basolateral side of IECs with their capacity to respond to lumenal PAMPs. TLR5 has been shown to be located on the basolateral membrane, which was suggested to be critical to limit overstimulation of IECs by the commensal bacterial components flagellin (Gewirtz et al., 2001). TLR2 and 4 have been described as being constitutively localized to the apical side of intestinal cells. Upon stimulation with LPS or peptiglycan, TLR2 and TLR4 have been seen to traffic to cellular compartments near the basolateral membrane (Cario et al., 2002, Hiemstra et al., 2015). It has been suggested that this trafficking is a mechanism used by IECs to transmit information from the lumen into underlying the immune cells of the lamina propria (Hiemstra et al., 2015). Additionally, TLR9 was shown to be located in both the apical and basolateral membranes but has been described to signal in a polarized manner. Basolateral stimulation of TLR9 leads to NFkB activation and the induction of an immune response however, apical stimulation leads to the ubiquitination of IkBa which causes it to accumulate therefore blocking apical signaling (Lee et al., 2006).

However, a recent study using transgenic mice expressing fluorescently labeled TLR 2, 4, 5, 7, and 9 has challenged many of these past models (Price et al., 2018). The current model suggests that to achieve homeostasis, which we define here as co-habitation of IECs with the commensal flora, TLRs are preferentially localized to specific sections in the GI tract as opposed to being polarized towards the basolateral side of epithelium cells. It was shown that TLR2, 4, and 5 were expressed at very low levels in the small intestine and at much higher levels in the colon. These three TLRs were found to be localized on both the apical and basolateral membranes. Interestingly, this study also showed

484 that TLR7 and 9 were absent from the epithelium and their expression was
485 limited to underlying immune cells. In such a model the longitudinal expression
486 patterns of TLRs along the GI tract might be adapted to the specific local
487 composition of the commensal flora and imbalances in their expression might
488 lead to the disruption of intestinal homeostasis. Alterations in the longitudinal
489 expression pattern of TLRs appears to be associated with pathologies and
490 sensitivity to enteric pathogens. It has been shown that suckling mice are more
491 susceptible to rotavirus infection due to low levels of TLR3. As mice age, they
492 increase TLR3 expression within the intestinal tract and become asymptomatic
493 to rotavirus infection (Pott et al., 2012). Adult mice which lack TLR3 or its
494 adapter TRIF increased their viral shedding and show a reduced immune
495 induction indicating that TLR3 is important for controlling viral pathogens in an
496 age-dependent manner. TLR5 and 4 have also been shown to be critical for
497 intestinal homeostasis. Mice lacking TLR5 expression display dysbiosis,
498 metabolic disorders, and low-grade inflammation of the intestinal tract. Using
499 intestinal specific knock-out of TLR5 it was shown that these symptoms were
500 based on the epithelial cells and not to underlying immune cells suggesting that
501 loss of TLR5 leads to an imbalance of the immune response generated in IECs
502 (Chassaing et al., 2014). Similarly, TLR4 overexpression leads to increased
503 severity of chemically induced colitis, increased inflammation and infiltration of
504 neutrophils. Additionally, TLR4 expression is associated with colitis-induced
505 cancers in human patients (Fukata et al., 2011).

506 To date no reports have directly visualized the distribution of TLR3
507 within the GI tract but sequencing data support a model where TLR3 is
508 expressed at similar levels in the different intestinal sections (Price et al., 2018,

509 Pott et al., 2012). As such is remains unclear whether or not TLR3 signaling is
510 specifically tailored to adapt to the challenges resulting from the commensal
511 flora/epithelium interface. In our work we clearly show that TLR3 displays a
512 polarized functionality independently of its location within the GI tract. We
513 found that basolateral infection leads to a stronger immune response in
514 organoids derived from duodenum, ileum and colon (Figure 3 and data not
515 shown). This demonstrate that IECs not only regulate expression and
516 downstream signal transduction of plasma membrane associated TLRs but also
517 endosomal TLRs.

518 We report that the clathrin sorting adaptor protein AP-1B is responsible
519 for the observed polarized immune response generated downstream TLR3. On
520 one hand AP-1B allows cells to mount a stronger immune response upon
521 basolateral viral infection and on the other hand it provides cells the capacity of
522 quickly downregulating the immune response upon apical viral challenges
523 (Figure 5). The function of clathrin adapter proteins in participating in the
524 regulation of TLR-mediated signaling was previously reported. Adapter protein
525 AP-3, has been shown to be critical for sorting of TLR 4 in DC and TLR7 and 9 in
526 pDCs (Mantegazza et al., 2012, Blasius et al., 2010). In the absence of AP-3 TLR7
527 and 9 are unable to produce type I IFN and TLR4s recruitment and signaling
528 from phagosomes is impaired, demonstrating that clathrin adapter protein
529 mediated sorting of TLRs directly influences the outcome of signal transduction.
530 Additionally, AP-1 sigma1c mutations have been found in patients that exhibit a
531 severe auto inflammatory skin disorder and it is suggested that this is due to
532 misregulation of the TLR3 receptor further supporting our model of a key role
533 for AP-1 in TLR3 signaling (Setta-Kaffetzi et al., 2014).

534 Interestingly we found that EMCV Mengo, which activates only RLRs,
535 transfected poly I:C and the STING agonist 2'3'cGAMP all elicited a polarized
536 immune induction which showed a higher induction of type I and III IFNs from
537 basolateral stimulation. This demonstrates that RLR signaling is also polarized in
538 IECs. By exploiting cells in which AP-1B was knocked-down we could show that
539 cells mount a strong immune response following TLR3 activation from the apical
540 infection. On the contrary, interfering with the AP-1B sorting machinery did not
541 alter neither RLR- nor STING- mediated signaling. This demonstrates that the
542 clathrin adapter AP-1B sorting machinery does not mediate the polarized
543 immune response generated by RLR or STING.

544 While it is clear that polarized RLRs are independent of AP-1B it is
545 unclear how cytosolic molecules could be polarized. Polarized cells are known to
546 organize their cytoplasm in a distinct architecture where the nucleus sits closer
547 to the basolateral membrane while the ER and the microtubule organizing center
548 are juxtaposed to the nucleus but facing the apical side. This suggest that the
549 physical nature of polarized cells could allow for segregating cytosolic
550 components involved in intrinsic innate immune sensing and signaling,
551 participating in the establishment of a polarized response. We have previously
552 shown that peroxisomes preferentially produce type III IFN (Odendall et al.,
553 2014). When evaluating the localization of peroxisomes in polarized cells we
554 could detect them dispersed through the basolateral cytosol but they were
555 excluded from the apical portion of the cell suggesting that they also show a
556 physical restriction allowing for their activation due to the delivery of
557 basolateral stimuli in a closer proximity to the sensors (data not shown).

Due to the challenge associated with the commensal microbiota/epithelium interface, IECs finely tune their intrinsic immune system. Regulation can be found at the quantitative level by selecting the expression of a subset of TLRs or can be achieved by creating a uniquely tailored response that allows for directional partial tolerance of commensals. We propose that in addition to plasma membrane-associated TLRs, IECs also functionally polarize intracellular and cytosolic PRRs. This polarization of function is intrinsically linked to the polarized nature of the cell and allows for TLR3, RLRs, and STING to strongly respond to basolateral challenges while limiting response to apical challenges (Figure 7). Importantly, AP-1B knock-out mice show an increase in inflammation and infiltration of CD4+ T cells due to an overreaction of IECs against the commensal flora (Takahashi et al., 2011). In the line with our results that AP-1B functionally polarizes PRR sensing and signaling, we propose that within the physiological organization of the gut, this side specific polarized immune response of IECs participates in the tolerance of the commensal flora located in the lumen while remaining responsive to invading pathogens that will gain access to the sterile basolateral side (Figure 7).

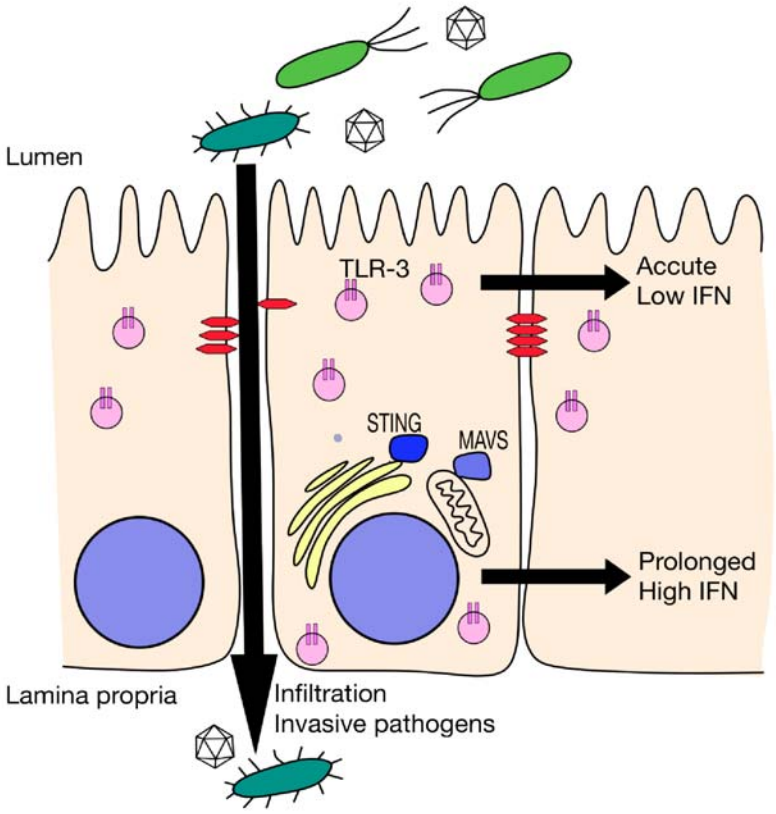

Figure 7. Apical stimulation is sensed by TLR3 and basolateral stimulation is sensed by a combination of TLR3 and RLR pathways. Model showing the acute, mild IFN sensing of commensal/pathogenic stimuli from the apical membrane compared to the high and prolonged IFN production from basolateral sensing after barrier breakdown/infiltration. Endosomes expressing TLR-3 are shown in pink, tight junctions are shown in red, ER-localized STING and mitochondrial MAVS are shown in blue.

576

Acknowledgments

This work was supported by a research grant from Chica and Heinz Schaller Foundation and Deutsche Forschungsgemeinschaft (DFG) in SFB1129 (Project 14) to SB. This project has received funding from the European Union's Seventh Framework Programme under grant agreement no 334336 (FP7-PEOPLE-2012-CIG). MS was supported by the Olympia Morata Fellowship from Heidelberg University Hospital, the Brigitte-Schlieben Lange Program from the state of Baden Württemberg, Germany and the Dual Career Support from CellNetworks, Heidelberg, Germany. We would like to thank Frank van Kuppeveld from Utrecht University for the EMCV Mengo virus.

Author Contributions

SB^a=Steeve Boulant , SB^b=Sina Bartfeld

MLS and SB^a designed experiments, MLS, SM, KP, MM and DA performed experiments, MLS analyzed data, TK and HO generated the KO mice organoids, CO and JK assisted in establishing polarized infection. SB^b designed and performed microinjection, MLS and SB^a wrote the manuscript. The final version of the manuscript was approved by all authors.

Declaration of Interests

The authors declare no competing interests.

References

ARPAIA, N. & BARTON, G. M. 2011. Toll-like receptors: key players in antiviral immunity. *Curr Opin Virol,* 1**,** 447-54.

BARTFELD, S. & CLEVERS, H. 2015. Organoids as Model for Infectious Diseases: Culture of Human and Murine Stomach Organoids and Microinjection of Helicobacter Pylori. *J Vis Exp*.

BARTON, G. M. & MEDZHITOV, R. 2003. Toll-like receptor signaling pathways. *Science,* 300**,** 1524-5.

BLASIUS, A. L., ARNOLD, C. N., GEORGEL, P., RUTSCHMANN, S., XIA, Y., LIN, P., ROSS, C., LI, X., SMART, N. G. & BEUTLER, B. 2010. Slc15a4, AP-3, and Hermansky-Pudlak syndrome proteins are required for Toll-like receptor signaling in plasmacytoid dendritic cells. *Proc Natl Acad Sci U S A,* 107**,** 19973-8.

BROERING, T. J., MCCUTCHEON, A. M., CENTONZE, V. E. & NIBERT, M. L. 2000. Reovirus nonstructural protein muNS binds to core particles but does not inhibit their transcription and capping activities. *J Virol,* 74**,** 5516-24.

CARIO, E., BROWN, D., MCKEE, M., LYNCH-DEVANEY, K., GERKEN, G. & PODOLSKY, D. K. 2002. Commensal-associated molecular patterns induce selective toll-like receptor-trafficking from apical membrane to cytoplasmic compartments in polarized intestinal epithelium. *Am J Pathol,* 160**,** 165-73.

CHASSAING, B., LEY, R. E. & GEWIRTZ, A. T. 2014. Intestinal epithelial cell toll-like receptor 5 regulates the intestinal microbiota to prevent low-grade inflammation and metabolic syndrome in mice. *Gastroenterology,* 147**,** 1363-77 e17.

CHOW, J., FRANZ, K. M. & KAGAN, J. C. 2015. PRRs are watching you: Localization of innate sensing and signaling regulators. *Virology,* 479-480**,** 104-9.

DE MATTEIS, M. A. & LUINI, A. 2008. Exiting the Golgi complex. *Nat Rev Mol Cell Biol,* 9**,** 273-84.

FENG, Q., HATO, S. V., LANGEREIS, M. A., ZOLL, J., VIRGEN-SLANE, R., PEISLEY, A., HUR, S., SEMLER, B. L., VAN RIJ, R. P. & VAN KUPPEVELD, F. J. 2012. MDA5 detects the double-stranded RNA replicative form in picornavirus-infected cells. *Cell Rep,* 2**,** 1187-96.

FOLSCH, H. 2015. Role of the epithelial cell-specific clathrin adaptor complex AP-1B in cell polarity. *Cell Logist,* 5**,** e1074331.

FUKATA, M. & ARDITI, M. 2013. The role of pattern recognition receptors in intestinal inflammation. *Mucosal Immunol,* 6**,** 451-63.

FUKATA, M., SHANG, L., SANTAOLALLA, R., SOTOLONGO, J., PASTORINI, C., ESPANA, C., UNGARO, R., HARPAZ, N., COOPER, H. S., ELSON, G., KOSCO-VILBOIS, M., ZAIAS, J., PEREZ, M. T., MAYER, L., VAMADEVAN, A. S., LIRA, S. A. & ABREU, M. T. 2011. Constitutive activation of epithelial TLR4 augments inflammatory responses to mucosal injury and drives colitis-associated tumorigenesis. *Inflamm Bowel Dis,* 17**,** 1464-73.

GEWIRTZ, A. T., NAVAS, T. A., LYONS, S., GODOWSKI, P. J. & MADARA, J. L. 2001. Cutting edge: bacterial flagellin activates basolaterally expressed TLR5 to induce epithelial proinflammatory gene expression. *J Immunol,* 167**,** 1882-5.

GONZALEZ, A. & RODRIGUEZ-BOULAN, E. 2009. Clathrin and AP1B: key roles in basolateral trafficking through trans-endosomal routes. *FEBS Lett,* 583**,** 3784-95.

HASE, K., NAKATSU, F., OHMAE, M., SUGIHARA, K., SHIODA, N., TAKAHASHI, D., OBATA, Y., FURUSAWA, Y., FUJIMURA, Y., YAMASHITA, T., FUKUDA, S., OKAMOTO, H., ASANO, M., YONEMURA, S. & OHNO, H. 2013. AP-1B-mediated protein sorting regulates polarity and proliferation of intestinal epithelial cells in mice. *Gastroenterology,* 145**,** 625-35.

HIEMSTRA, I. H., VRIJLAND, K., HOGENBOOM, M. M., BOUMA, G., KRAAL, G. & DEN HAAN, J. M. 2015. Intestinal epithelial cell transported TLR2 ligand stimulates Ly6C(+) monocyte differentiation in a G-CSF dependent manner. *Immunobiology,* 220**,** 1255-65.

KAGAN, J. C. & BARTON, G. M. 2014. Emerging principles governing signal transduction by pattern-recognition receptors. *Cold Spring Harb Perspect Biol,* 7**,** a016253.

KANAYA, T., SAKAKIBARA, S., JINNOHARA, T., HACHISUKA, M., TACHIBANA, N., HIDANO, S., KOBAYASHI, T., KIMURA, S., IWANAGA, T., NAKAGAWA, T., KATSUNO, T., KATO, N., AKIYAMA, T., SATO, T., WILLIAMS, I. R. & OHNO, H. 2018. Development of intestinal M cells and follicle-associated epithelium is regulated by TRAF6-mediated NF-kappaB signaling. *J Exp Med,* 215**,** 501-519.

LE BIVIC, A., REAL, F. X. & RODRIGUEZ-BOULAN, E. 1989. Vectorial targeting of apical and basolateral plasma membrane proteins in a human adenocarcinoma epithelial cell line. *Proc Natl Acad Sci U S A,* 86**,** 9313-7.

LEE, J., MO, J. H., KATAKURA, K., ALKALAY, I., RUCKER, A. N., LIU, Y. T., LEE, H. K., SHEN, C., COJOCARU, G., SHENOUDA, S., KAGNOFF, M., ECKMANN, L., BEN-NERIAH, Y. & RAZ, E. 2006. Maintenance of colonic homeostasis by distinctive apical TLR9 signalling in intestinal epithelial cells. *Nat Cell Biol,* 8**,** 1327-36.

LOO, Y. M., FORNEK, J., CROCHET, N., BAJWA, G., PERWITASARI, O., MARTINEZ-SOBRIDO, L., AKIRA, S., GILL, M. A., GARCIA-SASTRE, A., KATZE, M. G. & GALE, M., JR. 2008. Distinct RIG-I and MDA5 signaling by RNA viruses in innate immunity. *J Virol,* 82**,** 335-45.

MADARA, J. L., STAFFORD, J., DHARMSATHAPHORN, K. & CARLSON, S. 1987. Structural analysis of a human intestinal epithelial cell line. *Gastroenterology,* 92**,** 1133-45.

MANTEGAZZA, A. R., GUTTENTAG, S. H., EL-BENNA, J., SASAI, M., IWASAKI, A., SHEN, H., LAUFER, T. M. & MARKS, M. S. 2012. Adaptor protein-3 in dendritic cells facilitates phagosomal toll-like receptor signaling and antigen presentation to CD4(+) T cells. *Immunity,* 36**,** 782-94.

ODENDALL, C., DIXIT, E., STAVRU, F., BIERNE, H., FRANZ, K. M., DURBIN, A. F., BOULANT, S., GEHRKE, L., COSSART, P. & KAGAN, J. C. 2014. Diverse intracellular pathogens activate type III interferon expression from peroxisomes. *Nat Immunol,* 15**,** 717-26.

ODENDALL, C. & KAGAN, J. C. 2017. Activation and pathogenic manipulation of the sensors of the innate immune system. *Microbes Infect,* 19**,** 229-237.

PERVOLARAKI, K., STANIFER, M. L., MUNCHAU, S., RENN, L. A., ALBRECHT, D., KURZHALS, S., SENIS, E., GRIMM, D., SCHRODER-BRAUNSTEIN, J., RABIN, R. L. & BOULANT, S. 2017. Type I and Type III Interferons Display

695 Different Dependency on Mitogen-Activated Protein Kinases to Mount an
696 Antiviral State in the Human Gut. *Front Immunol,* 8**,** 459.
697 PETERSON, L. W. & ARTIS, D. 2014. Intestinal epithelial cells: regulators of
698 barrier function and immune homeostasis. *Nat Rev Immunol,* 14**,** 141-53.
699 POTT, J. & HORNEF, M. 2012. Innate immune signalling at the intestinal
700 epithelium in homeostasis and disease. *EMBO Rep,* 13**,** 684-98.
701 POTT, J., STOCKINGER, S., TOROW, N., SMOCZEK, A., LINDNER, C., MCINERNEY,
702 G., BACKHED, F., BAUMANN, U., PABST, O., BLEICH, A. & HORNEF, M. W.
703 2012. Age-dependent TLR3 expression of the intestinal epithelium
704 contributes to rotavirus susceptibility. *PLoS Pathog,* 8**,** e1002670.
705 PRICE, A. E., SHAMARDANI, K., LUGO, K. A., DEGUINE, J., ROBERTS, A. W., LEE, B.
706 L. & BARTON, G. M. 2018. A Map of Toll-like Receptor Expression in the
707 Intestinal Epithelium Reveals Distinct Spatial, Cell Type-Specific, and
708 Temporal Patterns. *Immunity,* 49**,** 560-575 e6.
709 RODRIGUEZ-BOULAN, E. & MACARA, I. G. 2014. Organization and execution of
710 the epithelial polarity programme. *Nat Rev Mol Cell Biol,* 15**,** 225-42.
711 SETTA-KAFFETZI, N., SIMPSON, M. A., NAVARINI, A. A., PATEL, V. M., LU, H. C.,
712 ALLEN, M. H., DUCKWORTH, M., BACHELEZ, H., BURDEN, A. D., CHOON, S.
713 E., GRIFFITHS, C. E., KIRBY, B., KOLIOS, A., SEYGER, M. M., PRINS, C.,
714 SMAHI, A., TREMBATH, R. C., FRATERNALI, F., SMITH, C. H., BARKER, J. N.
715 & CAPON, F. 2014. AP1S3 mutations are associated with pustular
716 psoriasis and impaired Toll-like receptor 3 trafficking. *Am J Hum Genet,*
717 94**,** 790-7.
718 STANIFER, M. L., KISCHNICK, C., RIPPERT, A., ALBRECHT, D. & BOULANT, S.
719 2017. Reovirus inhibits interferon production by sequestering IRF3 into
720 viral factories. *Sci Rep,* 7**,** 10873.
721 STANIFER, M. L., RIPPERT, A., KAZAKOV, A., WILLEMSEN, J., BUCHER, D.,
722 BENDER, S., BARTENSCHLAGER, R., BINDER, M. & BOULANT, S. 2016.
723 Reovirus intermediate subviral particles constitute a strategy to infect
724 intestinal epithelial cells by exploiting TGF-beta dependent pro-survival
725 signaling. *Cell Microbiol,* 18**,** 1831-1845.
726 STURZENBECKER, L. J., NIBERT, M., FURLONG, D. & FIELDS, B. N. 1987.
727 Intracellular digestion of reovirus particles requires a low pH and is an
728 essential step in the viral infectious cycle. *J Virol,* 61**,** 2351-61.
729 TAKAHASHI, D., HASE, K., KIMURA, S., NAKATSU, F., OHMAE, M., MANDAI, Y.,
730 SATO, T., DATE, Y., EBISAWA, M., KATO, T., OBATA, Y., FUKUDA, S.,
731 KAWAMURA, Y. I., DOHI, T., KATSUNO, T., YOKOSUKA, O., WAGURI, S. &
732 OHNO, H. 2011. The epithelia-specific membrane trafficking factor AP-1B
733 controls gut immune homeostasis in mice. *Gastroenterology,* 141**,** 621-32.
734 WEISZ, O. A. & RODRIGUEZ-BOULAN, E. 2009. Apical trafficking in epithelial
735 cells: signals, clusters and motors. *J Cell Sci,* 122**,** 4253-66.
736 WOLF, J. L., RUBIN, D. H., FINBERG, R., KAUFFMAN, R. S., SHARPE, A. H., TRIER, J.
737 S. & FIELDS, B. N. 1981. Intestinal M cells: a pathway for entry of reovirus
738 into the host. *Science,* 212**,** 471-2.
739 YAMAMOTO, M., SATO, S., HEMMI, H., HOSHINO, K., KAISHO, T., SANJO, H.,
740 TAKEUCHI, O., SUGIYAMA, M., OKABE, M., TAKEDA, K. & AKIRA, S. 2003.
741 Role of adaptor TRIF in the MyD88-independent toll-like receptor
742 signaling pathway. *Science,* 301**,** 640-3.

743 YU, S. & GAO, N. 2015. Compartmentalizing intestinal epithelial cell toll-like
744 receptors for immune surveillance. *Cell Mol Life Sci,* 72**,** 3343-53.
745
746

747 **STAR methods:**

748

749 **Cell and Viruses.** T84 human colon carcinoma cells (ATCC CCL-248) were
750 maintained in a 50:50 mixture of Dulbecco's modified Eagle's medium (DMEM)
751 and F12 (GibCo) supplemented with 10% fetal bovine serum and 1%
752 penicillin/streptomycin (Gibco). Reovirus strains Type 3 clone 9 (T3C9) derived
753 from stocks originally obtained from Bernard N. Fields were grown and purified
754 by standard protocols (Sturzenbecker et al., 1987). EMCV Mengo was a kind gift
755 from Frank van Kuppeveld (Utrecht University) and Salmonella
756 STm_14028_mCherry was a kind gift from Typas lab (EMBL Heidelberg).

757

758 **Antibodies and Inhibitors.** Rabbit polyclonal antibody against MRV uNS used at
759 1/1000 for immunostaining and western blots (Broering et al., 2000); ZO-1
760 (Santa Cruz Biotechnology) used at 1/100 for immunostaining; actin (Sigma-
761 Aldrich) used 1/2000 for western blots; J2 antibody was used at 1:250 for
762 detection of dsRNA. Secondary antibodies were conjugated with AF568
763 (Molecular Probes), CW800 (Li-Cor) or HRP (Sigma-Aldrich) directed against the
764 animal source. HMW and LMW poly I:C (Peprotech) were used in a 50:50 ratio at
765 a final concentration of 1 μg/mL and were delivered to the cells through
766 transfection as previously described (Stanifer et al., 2017). 2'3'-cGAMP
767 (Invivogen) was added directly to the media and was used at a final
768 concentration 10ug/mL. TRIF peptide inhibitor was used at a final concentration
769 of 25uM (Invivogen). Actinomycin D (Sigma) was used at a final concentration of
770 4ug/mL.

771

772 **Viral infections.** All MRV and EMCV infections were performed at an MOI of 1.
773 Media was removed from transwells and virus containing media was added to
774 either the apical or basolateral side. Virus was maintained for the course of the
775 experiment.
776
777 **Bacterial infection.** *Salmonella enterica serovar typhimurium* was streaked out
778 on a LB plate containing carbenicilin and incubate at 37˚C overnight. Single
779 colonies were picked and inoculated into LB carbenicilin liquid cultures and
780 were grown for 16h at 37˚C with shaking. The OD578 of the liquid culture was
781 read and then the samples were diluted 1:10 and incubated for an additional 4h
782 at 37˚C with shaking. OD578 was read every hour until reaching 1. Bacteria were
783 collected, spun at 8,000xg for 5 mins. Bacteria were washed in 1XPBS and spun
784 at 8,000xg for 5 mins. PBS was removed and bacteria were re-suspended in
785 DMEM +1g/L glucose in the absence of antibiotics to a allow for a final MOI of
786 100. Bacteria were added either apically or basolaterally to polarized T84 cells.
787 Infection was incubated at 37˚C for 30 mins. Bacteria were removed. Cells were
788 washed 1x with DMEM containing 100ug/mL gentamicin. Media was replaced
789 with DMEM containing gentamicin and samples were collected 8 hours post-
790 infection for analysis.
791
792 **Polarization of T84 cells on transwell inserts.** $1.2x10^5$ T84 cells were seeded
793 on polycarbonate transwell inserts (Corning, polycarbonate, 3.0 μM) in
794 DMEM/F12 medium. Medium was replaced 24h post-seeding and every two
795 days subsequently. The trans-epithelial electrical resistance (TEER) was tested
796 as indicated with EVOM^2 apparatus (World Precision Instrument). When the

797 TEER reached 1000 Ohm/cm^2, the T84 cells were considered polarized (Madara
798 et al., 1987). Polarization was controlled by immunostaining of the tight junction
799 protein ZO-1 (see indirect immunofluorescence assay).
800
801 **RNA isolation, cDNA, and qPCR**. RNA was harvested from cells using
802 NuceloSpin RNA extraction kit (Machery-Nagel) as per manufactures
803 instructions. cDNA was made using iSCRIPT reverse transcriptase (BioRad) from
804 250ng of total RNA as per manufactures instructions. q-RT-PCR was performed
805 using SsoAdvanced SYBR green (BioRad) as per manufacturer's instructions, TBP
806 and HPRT1 were used as normalizing genes.
807
808 **Western blot.** At time of harvest, media was removed, cells were rinsed one
809 time with 1X PBS and lysed with 1X RIPA (150 mM sodium chloride, 1.0% Triton
810 X-100, 0.5% sodium deoxycholate, 0.1% sodium dodecyl sulphate (SDS), 50 mM
811 Tris, pH 8.0 with phosphatase and protease inhibitors (Sigma-Aldrich)) for
812 5mins at RT. Lysates were collected and equal protein amounts were separated
813 by SDS-PAGE and blotted onto a nitrocellulose membrane by wet-blotting (Bio-
814 Rad, Germany). Membranes were blocked with 5% milk or 5% BSA in TBS
815 containing 0.1% Tween 20 (TBS-T) for one hour at room temperature. Primary
816 antibodies were diluted in blocking buffer and incubated overnight at 4°C.
817 Membranes were washed 3X in TBS-T for 5mins at RT. Secondary antibodies
818 were diluted in blocking buffer and incubated at RT for 1h with rocking.
819 Membranes were washed 3X in TBS-T for 5mins at RT. HRP detection reagent
820 (GE Healthcare) was mixed 1:1 and incubated at RT for 5mins. Membranes were
821 exposed to film and developed.

Indirect Immunofluorescence Assay. Polycarbonate transwell inserts were cut in half and fixed in 2% paraformaldehyde (PFA) for 20mins at room temperature (RT). Cells were washed and permeabilized in 0.5% Triton-X for 15 mins at RT. Primary antibodies were diluted in phosphate-buffered saline (PBS) and incubated for 1h at RT. Membranes were washed in 1X PBS three times and incubated with secondary antibodies for 45mins at RT. Membranes were washed in 1X PBS threes times and mounted on slides with ProLong Gold DAPI (Molecular Probes). Cells were imaged by epifluorescence on a Nikon Eclipse Ti-S (Nikon) or by confocal tile scans on a Zeiss LSM 780 (Zeiss). ZO-1 images were acquired on an ERS 6 spinning disc confocal microscope and deconvolution was performed using Huygens Remote Manager.

ELISA: Supernatants were collected at time points indicated in figure legends. Supernatants were kept undiluted. INFλ2/3 was evaluated using the INFλ 2/3 DIY ELISA (PBL Interferon source) for the basolateral supernatants only as we have previously shown that INFλ is preferentially secreted to the basolateral compartment (Stanifer et al., 2016). ELISA was performed as per manufacturers instructions.

Plaque Assay. BSC-1 were seeded into 24-well plates at a density of 200,000cells/well. 24-48h post-seeding when cells had reached 100% confluency, media was removed and cells were washed 1X with PBS+2mM $MgCl_2$ (PBS-M). Virus samples were harvested from infected T84 cells and were subject to three rounds of freezing and thawing. Samples were spun to remove cellular

847 debris and virus containing supernatants were diluted in 10-fold serial dilutions
848 in PBS-M. Infection was allowed to proceed for 1h at RT with rocking every
849 15mins. At the end of the incubation time, cells were overlaid with a 1:1 mixture
850 of 2% agarose:2X 199 Media (Sigma-Aldrich) containing 10u µg/mL
851 chymotrypsin. Cells were incubated at 37°C for 48h or until the appearance of
852 plaques. Cells were fixed in 10% formaldehyde for 30min at RT. Plugs were
853 removed and cells were stained with 0.5% crystal violet for 15min at RT. Crystal
854 violet was removed and cells were washed with water. Plaques were counted
855 and all samples were performed in triplicate.
856
857 **Dextran uptake assay.** 1 x 10^5 T84 cells were grown on collagen coated
858 transwell filters until reaching full polarization. At the indicated time the
859 diffusion of FITC-labelled dextran was measured. FITC-labeled dextran (Sigma-
860 Aldrich, 4 kDa) was to the apical surface at a final concentration of 2 mg/mL.
861 After incubating for 3h 37°C, 100 µL aliquots of the basal media were collected
862 and the fluorescence was measured with the FLUOstar Omega
863 spectrofluorometer (BMG Labtech) at 495 nm. As positive control, fluorescence
864 of 100 µL aliquot of a collagen coated but cell-free transwell filter was measured
865 to assess maximum diffusion of FITC-labeled dextran.
866
867 **Human organoid cultures.** Human tissue was received from colon and small
868 intestine resection from the University Hospital Heidelberg. This study was
869 carried out in accordance with the recommendations of the University hospital
870 Heidelberg with written informed consent from all subjects in accordance with
871 the Declaration of Helsinki. All samples were received and maintained in an

anonymized manner. The protocol was approved by the "Ethics commission of the University Hospital Heidelberg" under the protocol S-443/2017. Stem cells containing crypts were isolated following 2mM EDTA dissociation of tissue sample for 1hr at 4°C. Crypts were spun and washed in ice cold PBS. Fractions enriched in crypts were filtered with 70uM filters and the fractions were observed under a light microscope. Fractions containing the highest number of crypts were pooled and spun again. The supernatant was removed and crypts were re-suspended in Matrigel. Crypts were passaged and maintained in basal and differentiation culture media (see table 1).

Mouse organoids. Mouse intestinal tissue was received from control floxed mice or mice expressing a floxed Ap1m2 gene as previously described (Kanaya et al., 2018). Organoids were harvested, passaged and maintained in cultures as previously described for the human organoids, except using mouse specific media conditions (see table 1). To obtain organoids lacking the Ap1m2 gene, organoids were treated with 20uM tamoxifen for 48h. Tamoxifen was removed and cells were allowed to recover and grow in normal mouse media.

Microinjection. Human colon organoids were microinjected adapting a previously published protocol (Bartfeld and Clevers, 2015). Microinjection was carried out in a sterile laminar flow hood (KoJair, Finnland) using a micromanipulator (Narishige) and microinjector (Eppendorf FemtoJet). In each well, 30 organoids were injected. The injection needle was placed either inside the organoid (apical infection), or outside the organoid (basal infection), but

both time in similar proximity to the epithelium. Pairs of inside and outside injections were on the same plate.

Organoids on transwells. Tranwells were coated with 2.5% collagen in PBS for 1 hour prior to organoids seeding. Organoids were collected at a ratio of 100 organoids/transwell. Collected organoids were spun at 450g for 5mins and the supernatant was removed. Organoids were washed 1X with cold PBS and spun at 450g for 5mins. PBS was removed and organoids were digested with 0.5% Trypsin-EDTA (Life technologies) for 5 mins at 37°C. Digestion was stopped by addition of serum containing medium. Organoids were spun at 450g for 5mins and the supernatant was removed and organoids were re-suspended in normal growth media at a ratio of 100µL media/well. The PBS/matrigel mixture was removed from the transwells and 100 µL of organoids were added to each well. 500uL of normal organoid media was added to the bottom chambers. 24 hours post-seeding media on both sides of the transwells was changed for differentiation media and the TEER was monitored over 5 days.

RNA decay. T84 cells were seeded onto a 24-well plate at a density of 100,000cells/well. 24h post-seeding T84 cells were infected with MRV T3C9. 16 hours post-infection, cells were treated with 4 µg/mL actinomycin D and RNA samples were collected at time points indicated in figure legend. RNA was harvested and qPCR as performed as described above.

Production of Ap1 knock-down T84 cells. AP-1B knock-down T84 cells were seeded onto 6-well plates in a density of 500,000cells/well. 24h post-seeding

cells were transduced with lentiviruses expressing an shRNA targeted for the Ap1m2 gene (sequence available upon request). 72h post-transduction, lentiviruses were removed and T84 cells were put under antibiotic selection. When all control cells had died, antibiotic selection was removed and T84 cells were allowed to re-grow. Knock-down was confirmed through qPCR.

Statistics. Statistical analysis was performed using the GraphPad Prism software package. Unpaired t-tests were performed as described in the results section.

Table 1: Human and mouse media components

Compound	*Final concentration*
Human Basal media	
Ad DMEM/F12 +GlutaMAX +HEPES +P/S	
L-WRN conditioned media containing Wnt3A, R-spondin and Noggin	50% by volume
B27	1:50
N2	1:100
N-acetyl-cysteine	1mM
EGF	50ng/mL
Nicotinamide	10mM
A83-01	500nM
Sb202190	10uM
Differentiation Media	
Ad DMEM/F12 +GlutaMAX +HEPES +P/S	
B27	1:50
N2	1:100
N-acetyl-cysteine	1mM
R-spondin	5% by volume
Noggin	50ng/mL

EGF	50ng/mL
Gastrin	10mM
A83-01	500nM
Mouse Basal media	
Ad DMEM/F12 +GlutaMAX +HEPES +P/S	
B27	1:50
N2	1:100
R-spondin	10% by volume
Noggin	100ng/mL
EGF	50ng/mL

931